

Strongly anomalous diffusion in sheared magnetic configurations

E. Vanden Eijnden and R. Balescu

Association EURATOM-Etat Belge, Physique Statistique, Plasma et Optique NL C.P. 231,
Université Libre de Bruxelles, Campus Plaine, B-1050 Bruxelles, Belgium

(Received 17 May 1995; accepted 17 October 1995)

The statistical behavior of magnetic lines in a sheared magnetic configuration with reference surface $x=0$ is investigated within the framework of the kinetic theory. A Liouville equation is associated with the equations of motion of the stochastic magnetic lines. After averaging over an ensemble of realizations, it yields a convection-diffusion equation within the quasilinear approximation. The diffusion coefficients are space dependent and peaked around the reference surface $x=0$. Due to the shear, the diffusion of lines away from the reference surface is slowed down. The behavior of the lines is asymptotically strongly non-Gaussian. The reference surface acts like an attractor around which the magnetic lines spread with an effective subdiffusive behavior. Comparison is also made with more usual treatments based on the study of the first two moments equations. For sheared systems, it is explicitly shown that the Corrsin approximation assumed in the latter approach is no longer valid. It is also concluded that the diffusion coefficients cannot be derived from the mean square displacement of the magnetic lines in an inhomogeneous medium. © 1996 American Institute of Physics. [S1070-664X(96)00102-9]

I. INTRODUCTION

The description of turbulence phenomena in a high temperature plasma is a central issue for fusion. It has long been recognized, indeed, that classical transport theories based on the binary collisions assumption do not fully account for the behavior of a hot magnetized plasma.¹ Various other explanations have thus been proposed, among which magnetic turbulence appears as a plausible candidate.²⁻²⁵ Magnetic fluctuations, even very small, can highly disturb or even fully destroy the nested magnetic surfaces configuration which ensures confinement. In the latter case, the magnetic field is completely stochastic and a single magnetic line fills a three-dimensional region. This implies that the particles make important radial excursions, which drastically enhance the radial transport in the system yielding increasing leaks. Here, we restrict ourselves to the geometrical aspect of this problem without considering particle collisions. We thus describe the statistical properties of the magnetic lines alone.

In most studies devoted to magnetic turbulence,^{2-8,10-25} just like in the present paper, the magnetic fluctuations are given, i.e. the statistical properties of the field are specified from the start. Such a description is of course a simplification, and a more complete treatment would consider the field self-consistently. Here, it is assumed that the magnetic field observed in the laboratory reference frame (Eulerian picture) is a Gaussian random variable.^{13,17,24,25} Another simplification concerns the geometric modelisation of the system. A full description of a tokamak-like machine would require the use of rather complicated toroidal coordinates. We thus adopt the so-called slab approximation.^{4,5}

In comparison with a previous study,²⁵ however, we refine the model by including the shear,^{4,5,9,13,15,16,20} which is shown to have important effects. The presence of finite shear introduces a convection term in the equations of motion for the two components of the field lying in the plane $x-y$ perpendicular to the z -component of the main magnetic field. More precisely, any x -displacement gives rise to a displace-

ment along y which is of zeroth-order in the fluctuation. From a statistical point of view, such a convection mechanism has crucial consequences. It implies that the length of a magnetic line between two fixed z -values is greater in sheared than in shearless systems. Consequently, the two-point correlations of the magnetic field evaluated along a magnetic line (Lagrangian picture) vanish quicker in the presence of shear than in its absence.^{12,13,16} The "diffusion" of the lines is thus slowed down. Such an intuitive picture is however misleading, because it may yield two different interpretations. On one hand, one could expect that the behavior of the magnetic lines in a sheared configuration remains strictly diffusive, the effect of the shear being simply to reduce the diffusion coefficient. To the best of our knowledge, such a picture has been rather uniformly adopted in the plasma fusion literature.^{12,13,16} It should be noted, however, that the "strict-diffusion" picture does not exhaust the possibilities. Indeed, we show in this paper that the shear changes the *nature* of the process, yielding an effective *subdiffusive* behavior for the magnetic lines.

We will start by some discussions about the mathematical tools for describing the situation with shear. It will actually appear that the presence of shear requires to give up the Langevin description. The difficulties of the latter will be pointed out in Sec. II, where the model is presented; these difficulties are clearly related to the inhomogeneity introduced by the shear. In Sec. III, we introduce a Liouville equation for representing the motion of a magnetic line. This Liouville equation is averaged over an ensemble of realizations of the magnetic field, yielding a convection-diffusion equation whose coefficients are space-dependent. The importance of the latter point is underscored in Sec. IV: It is shown, indeed, that in such a case, the diffusion coefficient is not proportional to the second moment of the probability distribution function. In Sec. V, we derive a Smoluchowski equation by averaging the convection-diffusion equation over y : We thus restrict ourselves to a radial description (i.e.

along x) of the system. An analytical study of the Smoluchowski equation is performed and its results are compared to a direct numerical simulation. The solution is analyzed in Sec. VI, where various stages of diffusion are pointed out. Finally, concluding remarks are given in Sec. VII.

II. STATEMENT OF THE PROBLEM

The magnetic field considered in the present work is decomposed into an average part and a fluctuation. The average component contains a strong component conventionally directed along the z -axis of a Cartesian reference frame $\{x, y, z\}$ and a small component proportional to x along the y -axis representing the shear. The fluctuating part of the field lies in the $x-y$ plane,^{12,13}

$$\mathbf{B}(\mathbf{r}, z) = B_0 \{ \hat{\mathbf{z}} + x L_s^{-1} \hat{\mathbf{y}} + b_x(\mathbf{r}, z) \hat{\mathbf{x}} + b_y(\mathbf{r}, z) \hat{\mathbf{y}} \}, \quad (1)$$

where $\{\mathbf{r}\} = \{x, y\}$ and L_s is the shear length. Equation (1) should be understood as a local approximation, valid only in the neighborhood $|x| \ll L_s$ of the surface $x=0$ taken as a reference. In a more refined model (i.e. in toroidal geometry), the y and z coordinates would be replaced by poloidal and toroidal angular variables, respectively. In such a periodic model, there exist privileged surfaces; the rational surfaces. As shown for instance in Ref. 12, the sheared slab configuration defined by Eq. (1) is a local expansion in x around a rational surface with radial coordinate r_0 , valid for $r = r_0 + x$, with $|x| \ll r_0$. Despite this physical restriction, we underscore, however, that the $x L_s^{-1}$ term is of zeroth order compared to the fluctuation \mathbf{b} . The equations of a field line in three-dimensional (3-D) space are

$$\frac{dx}{B_0 b_x} = \frac{dy}{B_0 (b_y + x L_s^{-1})} = \frac{dz}{B_0}. \quad (2)$$

We take the z -coordinate as an independent variable playing the role of an effective time, and denote it by the Greek letter ζ . Equation (2) is equivalent to

$$\frac{dx}{d\zeta} = b_x[x(\zeta), y(\zeta); \zeta], \quad (3a)$$

$$\frac{dy}{d\zeta} = b_y[x(\zeta), y(\zeta); \zeta] + x(\zeta) L_s^{-1}. \quad (3b)$$

We complete the description of the model by specifying the statistical properties of the fluctuating magnetic field \mathbf{b} .^{24,25} The latter is assumed to be a centered Gaussian process, which is determined by its two-point correlation,

$$\mathcal{B}_{ij}(\mathbf{r}_1, \zeta_1 | \mathbf{r}_2; \zeta_2) = \langle b_i(\mathbf{r}_1; \zeta_1) b_j(\mathbf{r}_2; \zeta_2) \rangle, \quad (4a)$$

$$i = \{x, y\}; \quad j = \{x, y\}.$$

This tensor is assumed to be ‘‘stationary’’ in ζ and isotropic in the $x-y$ plane (i.e. *gyrotropic*) with the following exponential decay:

$$\begin{aligned} \mathcal{B}_{ij}(\mathbf{r} + \mathbf{r}'; \zeta + \zeta' | \mathbf{r}'; \zeta') \\ \equiv \mathcal{B}_{ij}(\mathbf{r}; \zeta) = \beta^2 \{ \delta_{ij} - \lambda_{\perp}^{-2} [r^2 \delta_{ij} - r_i r_j] \} \\ \times \exp \left(- \frac{\zeta^2}{2 \lambda_{\parallel}^2} - \frac{r^2}{2 \lambda_{\perp}^2} \right). \end{aligned} \quad (4b)$$

In spite of its apparent simplicity, the solution (in a statistical sense) of Eqs. (3) is a challenging problem. The difficulty can be pointed out immediately: In Eq. (4b), one has specified the correlation of the magnetic field when $\{x, y, \zeta\}$ are considered as independent variables. Such correlations, depending on x , y and ζ , are called Eulerian correlations. On the other hand, for the solution of Eqs. (3), it is necessary to know the correlations of the field when calculated along a trajectory $x(\zeta)$, $y(\zeta)$. Such correlations, depending on ζ alone, are called Lagrangian correlations. The determination of the Lagrangian from the Eulerian correlations (and *vice versa*) is a very complicated problem whose exact solution is, in general, impossible. One would like to begin the study of Eqs. (3) in a quite unusual but instructive way: We first show how apparently natural hypotheses can lead to wrong results. A widely used approximation for providing a link between Eulerian and Lagrangian correlations is the *Corrsin* (or independence) approximation.²⁴⁻²⁸ Within the latter one assumes, for instance,

$$\begin{aligned} \langle \mathbf{b}[\mathbf{r}(\zeta); \zeta] \rangle &= \int d\mathbf{r}_1 \langle \mathbf{b}[\mathbf{r}_1; \zeta] \delta[\mathbf{r}_1 - \mathbf{r}(\zeta)] \rangle \\ &\approx \int d\mathbf{r}_1 \langle \mathbf{b}[\mathbf{r}_1; \zeta] \rangle \langle \delta[\mathbf{r}_1 - \mathbf{r}(\zeta)] \rangle, \end{aligned} \quad (5)$$

(Corrsin).

The second step in Eq. (5) means that we approximate the field $\mathbf{b}[\mathbf{r}(\zeta); \zeta]$ by the field met by a particle that moves on the same path but *independently* from the magnetic field. In the present problem, Eq. (5) is, however, the source of a difficulty. We have indeed assumed that the Eulerian average of \mathbf{b} vanishes. Equation (5) would then imply that the Lagrangian average of \mathbf{b} also vanishes. Hence, we would conclude from Eqs. (3) that

$$\langle x(\zeta) \rangle = x_0, \quad \langle y(\zeta) \rangle = y_0 + x_0 L_s^{-1} \zeta, \quad (6)$$

where $x_0 = x(0)$ and $y_0 = y(0)$ are the deterministic initial conditions. Equations (3) can then be transformed into equations for the deviations $\delta \mathbf{r}(\zeta) = \mathbf{r}(\zeta) - \langle \mathbf{r}(\zeta) \rangle$. If the magnetic perturbation is weak, one can take into account only the leading influence of \mathbf{b} (quasilinear approximation). It yields, for instance for Eq. (3a),

$$\frac{d}{d\zeta} \delta x(\zeta) = b_x[x(\zeta), y(\zeta); \zeta] \approx b_x[\langle x(\zeta) \rangle, \langle y(\zeta) \rangle; \zeta].$$

This equation is readily integrated using Eq. (6) and the mean square displacement would then yield [using (4a)]

$$\begin{aligned} \langle \delta x^2(\zeta) \rangle &= x_0^2 + \int_0^{\zeta} d\zeta_1 \int_0^{\zeta_1} d\zeta_2 \\ &\times \mathcal{B}_{xx}(0, x_0 L_s^{-1} (\zeta_1 - \zeta_2); \zeta_1 - \zeta_2), \end{aligned} \quad (7)$$

and hence [using (4b)]

$$\frac{1}{2} \lim_{\zeta \rightarrow \infty} \frac{d}{d\zeta} \langle \delta x^2(\zeta) \rangle = \sqrt{\frac{\pi}{2}} \beta^2 \lambda_{\parallel} \left[1 + \frac{\lambda_{\parallel}^2 x_0^2}{\lambda_{\perp}^2 L_s^2} \right]^{-3/2}. \quad (8)$$

Although this formula gives the well-known quasilinear limit for the shearless case ($L_s \rightarrow \infty$),^{6,8,12,13,24,25} it exhibits contra-

dictory features when L_s is finite: On one hand, Eq. (7) implies that the process is diffusive, i.e. that the mean square deviation (MSD) grows linearly in time ζ when ζ goes to infinity. But, on the other hand, the diffusion coefficient $D_m = \frac{1}{2} \lim_{\zeta \rightarrow \infty} (d/d\zeta) \langle \delta x^2(\zeta) \rangle$ in Eq. (7) depends on the initial condition x_0 . Hence, according to Eq. (7), a magnetic line located initially in x_0 can be found on the average in a region whose spreading grows more and more up to infinity, but whose growth rate for all times depends on the initial position of the line. This memory effect does not correspond to the actual physics and spuriously comes from the very first approximation (5): If taken *along the trajectory* (Lagrangian picture), the mean of the fluctuating part of the magnetic field is not necessarily zero, i.e. $\langle \mathbf{b}[\mathbf{r}(\zeta); \zeta] \rangle \neq 0$, and hence $\langle x(\zeta) \rangle \neq x_0$ and $\langle y(\zeta) \rangle \neq y_0 + x_0 L_s^{-1} \zeta$. Such a property is well known even for very simple systems; nonlinear equations like Eqs. (3) can produce so called *noise induced drifts*.^{29–32} Consequently, the Corrsin approximation (5) is not appropriate to the present problem. The right way is based on a kinetic treatment of Eqs. (3).²⁹

III. THE CONVECTION-DIFFUSION EQUATION IN THE QUASILINEAR LIMIT

The stochastic Liouville equation associated with Eqs. (3) is^{2,12,23,25,33}

$$\partial_\zeta f(\mathbf{r}; \zeta) + x L_s^{-1} \nabla_y f(\mathbf{r}; \zeta) + \mathbf{b}(\mathbf{r}; \zeta) \cdot \nabla f(\mathbf{r}; \zeta) = 0, \quad (9)$$

where f is the probability distribution function (PDF) on the phase space $\{\mathbf{r}\} = \{x, y\}$. We take as initial condition $f(\mathbf{r}; 0) = \delta(\mathbf{r} - \mathbf{r}_0)$. Equation (9) is thus totally equivalent to Eqs. (3), which implies $f(\mathbf{r}; \zeta) = \delta[\mathbf{r} - \mathbf{r}(\zeta)]$, where $\mathbf{r}(\zeta)$ is the solution of Eqs. (3). As usual, we split the PDF into an average and a fluctuating part,

$$f = F + \delta f, \quad F = \langle f \rangle, \quad \langle \delta f \rangle = 0.$$

They obey the following equations:

$$\partial_\zeta F + x L_s^{-1} \nabla_y F + \nabla \cdot \langle \mathbf{b} \delta f \rangle = 0, \quad (10a)$$

$$\partial_\zeta \delta f + x L_s^{-1} \nabla_y \delta f + \nabla \cdot \mathbf{b} F + \nabla \cdot \{ \mathbf{b} \delta f - \langle \mathbf{b} \delta f \rangle \} = 0, \quad (10b)$$

where we have used the zero divergence constraint $\nabla \cdot \mathbf{b} = 0$. The unperturbed propagator of Eqs. (10) is the solution of

$$\partial_{\zeta_1} g_0(\mathbf{r}_1; \zeta_1 | \mathbf{r}_2; \zeta_2) + x_1 L_s^{-1} \nabla_{y_1} g_0(\mathbf{r}_1; \zeta_1 | \mathbf{r}_2; \zeta_2) = 0, \quad (11)$$

with initial condition $g_0(\mathbf{r}_1; \zeta_1 | \mathbf{r}_2; \zeta) = \delta(\mathbf{r}_1 - \mathbf{r}_2)$. It yields

$$g_0(\mathbf{r}_1; \zeta_1 | \mathbf{r}_2; \zeta_2) = \delta[x_1 - x_2] \delta[y_1 - x_1 L_s^{-1} (\zeta_1 - \zeta_2) - y_2]. \quad (12)$$

Here we solve Eq. (10b) within the quasilinear, or Bourret, approximation^{2,12,13,29,34,35} and neglect the term $\nabla \cdot \{ \mathbf{b} \delta f - \langle \mathbf{b} \delta f \rangle \}$ in Eq. (10b). The validity of this approximation requires, as shown in Refs. 24 and 35, that

$$\alpha = \beta \lambda_{\parallel} \lambda_{\perp}^{-1} \ll 1,$$

where α is usually called the Kubo number. Within the quasilinear approximation, the solution of Eq. (10b) with initial condition $\delta f(\mathbf{r}; 0) = 0$ is thus

$$\begin{aligned} \delta f(\mathbf{r}; \zeta) = & - \int_0^\zeta d\zeta' \int d\mathbf{r}' g_0(\mathbf{r}; \zeta | \mathbf{r}'; \zeta') \\ & \times \nabla' \cdot \mathbf{b}(\mathbf{r}'; \zeta') F(\mathbf{r}'; \zeta'). \end{aligned} \quad (13)$$

By injecting this solution in Eq. (10a) and using Eq. (12), we obtain

$$\begin{aligned} \partial_\zeta F(\mathbf{r}; \zeta) + x L_s^{-1} \nabla_y F(\mathbf{r}; \zeta) \\ = \sum_{ij} \int_0^\zeta d\zeta' \nabla_i \langle b_i(x, y; \zeta) b_j(x, y - x L_s^{-1} \zeta'; \zeta - \zeta') \rangle \\ \times \hat{\nabla}_j F(x, y - x L_s^{-1} \zeta'; \zeta - \zeta'), \end{aligned} \quad (14a)$$

where the operator $\hat{\nabla}$ is defined by

$$\hat{\nabla}_x = \nabla_x + L_s^{-1} \zeta' \nabla_y, \quad \hat{\nabla}_y = \nabla_y. \quad (14b)$$

In the quasilinear approximation, the ζ -displacement of the PDF appearing in the right hand side of Eq. (14a) is determined by the unperturbed propagator: $F(\mathbf{r}; \zeta) \approx \int d\mathbf{r}' g_0(\mathbf{r}; \zeta | \mathbf{r}'; \zeta') F(\mathbf{r}'; \zeta')$. This statement implies, taking in Eq. (14a)

$$F(x, y - x L_s^{-1} \zeta'; \zeta - \zeta') \approx F(x, y; \zeta). \quad (15)$$

We shall be mainly interested in the asymptotic (large ζ) behavior of F : We therefore extend the integration over ζ' up to infinity in Eq. (14a). Finally, using Eqs. (4), Eq. (14a) simplifies into the *convection-diffusion equation* (or “nonlinear” Fokker–Planck equation²⁹)

$$\partial_\zeta F(x, y; \zeta) + x L_s^{-1} \nabla_y F(x, y; \zeta) = \nabla \cdot \mathcal{D}(x) \cdot \nabla F(x, y; \zeta), \quad (16)$$

where the (nonsymmetric) diffusion tensor $\mathcal{D}(x)$ is

$$\mathcal{D}_{xx}(x) = \sqrt{\frac{\pi}{2}} \beta^2 \lambda_{\parallel} \left[1 + \frac{\theta_s^2 x^2}{\lambda_{\perp}^2} \right]^{-3/2}, \quad (17a)$$

$$\begin{aligned} \mathcal{D}_{xy}(x) = \beta^2 \lambda_{\parallel}^2 L_s^{-1} \left[1 - \frac{\theta_s^2 x^2}{\lambda_{\perp}^2} \right] \left[1 + \frac{\theta_s^2 x^2}{\lambda_{\perp}^2} \right]^{-2}, \\ \mathcal{D}_{yx} = 0, \end{aligned} \quad (17b)$$

$$\mathcal{D}_{yy}(x) = \sqrt{\frac{\pi}{2}} \beta^2 \lambda_{\parallel} \left[1 + \frac{\theta_s^2 x^2}{\lambda_{\perp}^2} \right]^{-1/2}, \quad (17c)$$

where $\theta_s = \lambda_{\parallel} L_s^{-1}$. The x -dependence of the diffusion tensor $\mathcal{D}(x)$ follows from the privileged role played by the surface $x=0$ in our model. It shows that this surface influences the statistical properties of the fluctuations in its neighborhood. It must also be stressed that the x -dependence of $\mathcal{D}(x)$ is a consequence of the magnetic field correlation (4b). In any non-self-consistent theory of magnetic fluctuations (such as ours, and as most other existing treatments), there is an element of arbitrariness in the choice of the statistics of the fluctuating field. We believe that our choice (4b) is physically sensible, as expressing a natural gyrotropy (the same choice appears in Ref. 13). The shear produces a rotation effect on the correlation function, but this is clearly accounted for in our treatment by the action of the propagator

$g_0(\mathbf{r}; \boldsymbol{\zeta} | \mathbf{r}'; \boldsymbol{\zeta}')$ [see, e.g., Eq. (13)]. One could have chosen a different correlation function incorporating the rotation effect, such as

$$\langle b_i(\mathbf{r}_1; \boldsymbol{\zeta}_1) b_j(\mathbf{r}_2; \boldsymbol{\zeta}_2) \rangle \equiv \mathcal{B}_{ij}(x_1 - x_2, y_1 - y_2 - L_s^{-1}[x_1 \zeta_1 - x_2 \zeta_2]; \boldsymbol{\zeta}_1 - \boldsymbol{\zeta}_2).$$

In this case the action of g_0 annuls the effect, and one finds a constant diffusion tensor as in the shearless case [actually, Eqs. (17) for $x=0$]. We believe, however, that this results from a double-counting of the rotation effect.

Finally, let us compare the results of this section with those obtained by using the Corrsin approximation (see Sec. II): Using Eqs. (10a) and (16), one first notes that the quasilinear approximation implies

$$\langle \mathbf{b}(\mathbf{r}; \boldsymbol{\zeta}) \delta f(\mathbf{r}; \boldsymbol{\zeta}) \rangle = -\mathcal{D}(x) \cdot \nabla F(\mathbf{r}; \boldsymbol{\zeta}).$$

One thus gets for the Lagrangian correlation of the magnetic field [see Eq. (5)]

$$\begin{aligned} \langle \mathbf{b}(\mathbf{r}(\boldsymbol{\zeta}); \boldsymbol{\zeta}) \rangle &\equiv \int d\mathbf{r} \langle \mathbf{b}(\mathbf{r}; \boldsymbol{\zeta}) \delta f(\mathbf{r}; \boldsymbol{\zeta}) \rangle \\ &= \int d\mathbf{r} (\nabla \cdot \mathcal{D}^T(x)) F(\mathbf{r}; \boldsymbol{\zeta}), \end{aligned} \quad (18)$$

where \mathcal{D}^T is the transposed of \mathcal{D} . In the shearless case ($L_s \rightarrow \infty$), the x -dependence of the diffusion tensor disappears, i.e. $\mathcal{D}_{ij}(x) \rightarrow \sqrt{\pi/2} \beta^2 \lambda_{\parallel} \delta_{ij}$. From Eq. (18), one thus sees that the Lagrangian correlation of \mathbf{b} is zero if $L_s \rightarrow \infty$. It justifies the Corrsin approximation in the shearless system. However, this argument fails for finite shear, i.e. when $\mathcal{D}(x)$ depends on x . According to Eq. (18), the Lagrangian correlation of \mathbf{b} is nonzero in a sheared system. More precisely, Eq. (18) implies

$$\langle b_x(\mathbf{r}(\boldsymbol{\zeta}); \boldsymbol{\zeta}) \rangle \neq 0, \quad \langle b_y(\mathbf{r}(\boldsymbol{\zeta}); \boldsymbol{\zeta}) \rangle = 0. \quad (19)$$

Consequently, the quasilinear kinetic treatment presented here goes beyond the Corrsin-based treatment given in Sec. II [see Eqs. (5-8)]. In some sense, it gives an estimation for the accuracy of the Corrsin approximation, which is shown to miss the inhomogeneous character of the process.

IV. KINETIC EQUATION VERSUS MOMENTS EQUATIONS

Let us consider a general advection-diffusion equation like Eq. (16),

$$\partial_{\boldsymbol{\zeta}} F(\mathbf{r}; \boldsymbol{\zeta}) + \nabla \cdot \mathbf{u}(\mathbf{r}; \boldsymbol{\zeta}) F(\mathbf{r}; \boldsymbol{\zeta}) = \nabla \cdot \mathcal{D}(\mathbf{r}; \boldsymbol{\zeta}) \cdot \nabla F(\mathbf{r}; \boldsymbol{\zeta}), \quad (20)$$

with $\nabla \cdot \mathbf{u} = 0$. In this section, we are interested in the following question: Under which conditions about the drift vector \mathbf{u} and diffusion tensor \mathcal{D} , can we derive from Eq. (20) a closed set of equations for the first two moments of the PDF? The latter are defined by

$$\boldsymbol{\mu}(\boldsymbol{\zeta}) = \int d\mathbf{r} \mathbf{r} F(\mathbf{r}; \boldsymbol{\zeta}), \quad (21a)$$

$$\Gamma(\boldsymbol{\zeta}) = \int d\mathbf{r} [\mathbf{r} - \boldsymbol{\mu}(\boldsymbol{\zeta})][\mathbf{r} - \boldsymbol{\mu}(\boldsymbol{\zeta})] F(\mathbf{r}; \boldsymbol{\zeta}). \quad (21b)$$

The previous question is important because the Langevin approach focuses on these first two moments. From Eqs. (20) and (21a), one gets

$$\begin{aligned} \partial_{\boldsymbol{\zeta}} \boldsymbol{\mu}(\boldsymbol{\zeta}) &= \int d\mathbf{r} \mathbf{u}(\mathbf{r}; \boldsymbol{\zeta}) F(\mathbf{r}; \boldsymbol{\zeta}) \\ &+ \int d\mathbf{r} (\nabla \cdot \mathcal{D}^T(\mathbf{r}; \boldsymbol{\zeta})) F(\mathbf{r}; \boldsymbol{\zeta}), \end{aligned} \quad (22)$$

with initial condition $\boldsymbol{\mu}(0) = \boldsymbol{\mu}_0$. Obviously, for general \mathbf{u} and \mathcal{D} , Eq. (22) is not a closed equation. Its complication is due to the \mathbf{r} -dependence of the coefficients in Eq. (20). Whenever $\mathbf{u}(\mathbf{r}; \boldsymbol{\zeta}) = \mathbf{u}(\boldsymbol{\zeta})$ and $\mathcal{D}(\mathbf{r}; \boldsymbol{\zeta}) = \mathcal{D}(\boldsymbol{\zeta})$, Eq. (22) reduces to

$$\partial_{\boldsymbol{\zeta}} \boldsymbol{\mu}(\boldsymbol{\zeta}) = \mathbf{u}(\boldsymbol{\zeta}), \quad \boldsymbol{\mu}(\boldsymbol{\zeta}) = \boldsymbol{\mu}_0 + \int_0^{\boldsymbol{\zeta}} d\boldsymbol{\zeta}' \mathbf{u}(\boldsymbol{\zeta}'). \quad (23)$$

More important yet is the equation for the second moment. From Eqs. (20) and (21b), we obtain

$$\begin{aligned} \partial_{\boldsymbol{\zeta}} \Gamma_{mn}(\boldsymbol{\zeta}) &= \int d\mathbf{r} \{ [r_m - \mu_m(\boldsymbol{\zeta})] u_n(\mathbf{r}; \boldsymbol{\zeta}) \\ &+ [r_n - \mu_n(\boldsymbol{\zeta})] u_m(\mathbf{r}; \boldsymbol{\zeta}) \} F(\mathbf{r}; \boldsymbol{\zeta}) \\ &+ \sum_i \int d\mathbf{r} \nabla_i \{ [r_m - \mu_m(\boldsymbol{\zeta})] \mathcal{D}_{ni}(\mathbf{r}; \boldsymbol{\zeta}) \\ &+ [r_n - \mu_n(\boldsymbol{\zeta})] \mathcal{D}_{mi}(\mathbf{r}; \boldsymbol{\zeta}) \} F(\mathbf{r}; \boldsymbol{\zeta}), \end{aligned} \quad (24)$$

with initial condition $\Gamma_{mn}(0) = 0$. Consider, in particular, the mean square displacement $\langle \delta r^2(\boldsymbol{\zeta}) \rangle \equiv \text{Tr} \Gamma(\boldsymbol{\zeta})$, which is traditionally used for the calculation of the diffusion coefficient in all theories based on the Langevin equation. Combining Eqs. (22) and (24) we find

$$\begin{aligned} \partial_{\boldsymbol{\zeta}} \langle \delta r^2(\boldsymbol{\zeta}) \rangle &= 2 \sum_j \left\{ \int d\mathbf{r} r_j u_j(\mathbf{r}; \boldsymbol{\zeta}) F(\mathbf{r}; \boldsymbol{\zeta}) \right. \\ &- \mu_j(\boldsymbol{\zeta}) \int d\mathbf{r} u_j(\mathbf{r}; \boldsymbol{\zeta}) F(\mathbf{r}; \boldsymbol{\zeta}) \left. \right\} \\ &+ 2 \sum_{jn} \left\{ \int d\mathbf{r} r_j (\nabla_n \mathcal{D}_{jn}(\mathbf{r}; \boldsymbol{\zeta})) F(\mathbf{r}; \boldsymbol{\zeta}) \right. \\ &- \mu_j(\boldsymbol{\zeta}) \int d\mathbf{r} (\nabla_n \mathcal{D}_{jn}(\mathbf{r}; \boldsymbol{\zeta})) F(\mathbf{r}; \boldsymbol{\zeta}) \left. \right\} \\ &+ 2 \sum_n \int d\mathbf{r} \mathcal{D}_{nn}(\mathbf{r}; \boldsymbol{\zeta}) F(\mathbf{r}; \boldsymbol{\zeta}). \end{aligned} \quad (25)$$

It is now clearly seen again that the complication of this equation is due to the space dependence. When $\mathbf{u}(\mathbf{r}; \boldsymbol{\zeta}) = \mathbf{u}(\boldsymbol{\zeta})$, the first two terms in the right hand side cancel each other. When, moreover, $\mathcal{D}_{jn}(\mathbf{r}; \boldsymbol{\zeta}) = \mathcal{D}_{jn}(\boldsymbol{\zeta})$, the next two terms vanish and we are left with

$$\partial_{\boldsymbol{\zeta}} \langle \delta r^2(\boldsymbol{\zeta}) \rangle = 2 \text{Tr} \mathcal{D}(\boldsymbol{\zeta}). \quad (26)$$

$\text{Tr} \mathcal{D}(\boldsymbol{\zeta})$ is thus identified with the running diffusion coefficient. If the system is gyrotropic, $\mathcal{D}_{mn}(\boldsymbol{\zeta}) = D(\boldsymbol{\zeta}) \delta_{mn}$, and if its behavior is truly diffusive [$\lim_{\boldsymbol{\zeta} \rightarrow \infty} D(\boldsymbol{\zeta}) = D > 0$], then we find the usual relation between the mean square displacement and the diffusion coefficient,

$$D = \frac{1}{2d} \lim_{\zeta \rightarrow \infty} \partial_{\zeta} \langle \delta r^2(\zeta) \rangle, \quad (27)$$

where d is the dimensionality. The comparison between Eqs. (25) and (26) or (27) should be a warning against the use of the “standard” definition of the diffusion coefficient in situations where it is not valid. In particular, Eq. (16) clearly shows that \mathbf{u} and \mathcal{D} are both space-dependent in a sheared magnetic field, hence Eq. (27) is invalid.

V. THE SMOLUCHOWSKI EQUATION

Both theoretically and for the problem of radial transport in a tokamak, the interesting part of the PDF F comes from its x -dependence. We thus restrict the study of Eq. (16) to the x -variable by integrating this equation over y . In the dimensionless variables $\hat{\mathbf{r}} = \mathbf{r}\lambda_{\perp}^{-1}$ and $\tau = \zeta\lambda_{\parallel}^{-1}$, Eqs. (16) and (17) become

$$\partial_{\tau} n = \nabla_{\hat{x}} (D(\theta_s \hat{x}) \nabla_{\hat{x}} n), \quad (28)$$

where

$$n(\hat{x}; \tau) = \lambda_{\perp}^2 \int_{-\infty}^{\infty} d\hat{y} F(\lambda_{\perp} \hat{x}, \lambda_{\perp} \hat{y}; \lambda_{\parallel} \tau) \quad (29)$$

and

$$D(\theta_s \hat{x}) = d_m [1 + \theta_s^2 \hat{x}^2]^{-3/2}, \quad (30a)$$

$$d_m = \sqrt{\frac{\pi}{2}} \beta^2 \lambda_{\parallel}^2 \lambda_{\perp}^{-2}. \quad (30b)$$

Here $n(\hat{x}; \tau)$ is appropriately called the density profile; d_m is the well-known quasilinear magnetic line diffusion coefficient in the shearless limit.^{6,8,12,13,24,25} In this section we perform an analytical study of Eq. (28) in the range $\theta_s \lesssim 1$, and we compare the results to a direct numerical solution. The analytical study proceeds as follows: First, we introduce the new variable (from here on we suppress the hat on the dimensionless variable \hat{x})³¹,

$$\eta = \int_{x_0}^x dp [1 + \theta_s^2 p^2]^{3/4}. \quad (31)$$

Equation (28) becomes the Smoluchowski equation,^{31,36}

$$\partial_{\tau} \bar{n} = -\nabla_{\eta} (V \bar{n}) + d_m \nabla_{\eta}^2 \bar{n}, \quad (32)$$

where $\bar{n}(\eta; \tau) = [1 + \theta_s^2 x^2]^{-3/4} n(x; \tau)|_{x=x(\eta)}$. Boundary and initial conditions are $\bar{n}(\pm\infty; \tau) = 0$ and $\bar{n}(\eta; 0) = \delta(\eta)$. The drift coefficient V is

$$V(\eta) = -\frac{3}{2} d_m \theta_s^2 x [1 + \theta_s^2 x^2]_{|x=x(\eta)}^{-7/4}. \quad (33)$$

When $\theta_s \lesssim 1$, the drift term in Eq. (32) is a small correction. One thus introduces the decomposition,³⁷

$$\bar{n} = \bar{n}_0 + \bar{n}_1, \quad (34)$$

and, neglecting higher order terms, we split Eq. (32) into

$$\partial_{\tau} \bar{n}_0 = d_m \nabla_{\eta}^2 \bar{n}_0, \quad (35a)$$

$$\partial_{\tau} \bar{n}_1 = d_m \nabla_{\eta}^2 \bar{n}_1 - \nabla_{\eta} (V \bar{n}_0). \quad (35b)$$

The solution of Eq. (35a) is

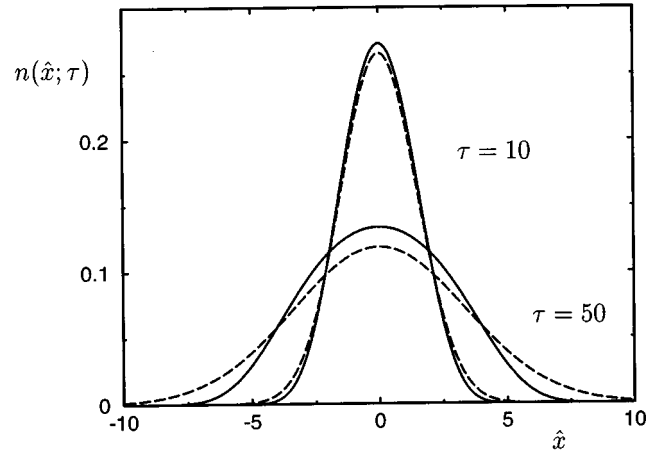


FIG. 1. The numerical solution of Eq. (28) and the density profile (37) (full lines) are compared with the shearless (Gaussian packet) solution (dashed lines) for $\hat{x}_0=0$. Upper curves $\tau=10$; lower curves $\tau=50$ ($\theta_s=0.2$ and $\alpha=0.3$). Equation (37) fits perfectly the numerical data. Moreover, the deviations from Gaussianity are weak, even for rather large values of τ .

$$\bar{n}_0(\eta; \tau) = (4\pi d_m \tau)^{-1/2} \exp\left(-\frac{\eta^2}{4 d_m \tau}\right). \quad (36a)$$

The expression (36a) is the Green function of Eq. (35b), which yields

$$\begin{aligned} \bar{n}_1(\eta; \tau) = & -\int_0^{\tau} d\tau' \int_{-\infty}^{\infty} d\eta' \bar{n}_0(\eta - \eta'; \tau - \tau') \\ & \times \nabla_{\eta'} (V(\eta') \bar{n}_0(\eta'; \tau')). \end{aligned} \quad (36b)$$

Finally, going back to the variable x , Eqs. (36a) and (36b) can be combined into a single expression which reduces, after some straightforward algebra, to

$$\begin{aligned} n(x; \tau) = & (4\pi D(\theta_s x) \tau)^{-1/2} \left\{ \left(1 - \frac{3}{4} \ln[1 + \theta_s^2 x^2] \right) \right. \\ & \times \exp\left(-\frac{1}{4 d_m \tau} \eta^2(x)\right) + \frac{3}{8} (d_m \tau)^{-1} \\ & \times \left(\int_{-\infty}^x - \int_{x_0}^{\infty} \right) dx' [1 + \theta_s^2 x'^2]^{3/4} \\ & \times \ln[1 + \theta_s^2 x'^2] (\eta(x) - 2\eta(x')) \\ & \left. \times \exp\left(-\frac{1}{4 d_m \tau} [\eta(x) - 2\eta(x')]^2\right) \right\}. \end{aligned} \quad (37)$$

The latter expression is plotted in Figs. 1–4: It will be analyzed in Sec. VI. For times that are not too long (this will be precisely defined in Sec. VI B) and for $\theta_s \lesssim 1$, Eq. (37) very accurately approximates the exact solution of Eq. (32) (see Figs. 1 and 2). However, Eq. (37) contains secularities and breaks down for very large times (see Figs. 3 and 4). More precisely, this occurs when the solution of Eq. (32) has spread over a large x -range. In the latter case, an approximation for the solution of Eq. (32) can be obtained as follows³⁸: First, we note that

$$\eta \sim \frac{2}{5} \theta_s^{3/2} |x|^{5/2} \text{sgn}(x), \quad \theta_s x \gg 1 \text{ and } x \gg x_0. \quad (38)$$

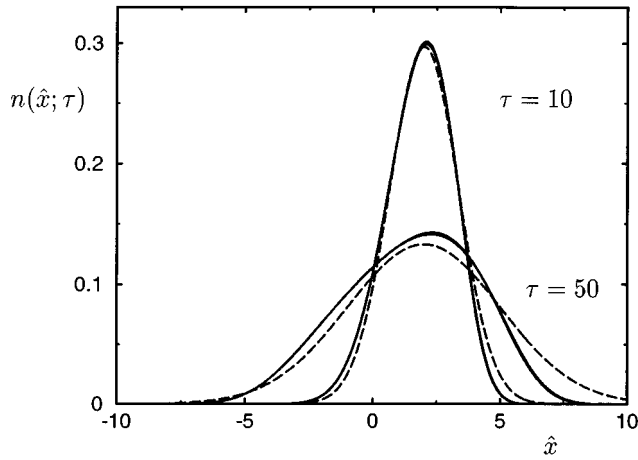


FIG. 2. The numerical solution of Eq. (28) and the density profile (37) (full lines) are compared with the local Gaussian packet solution (dashed lines) for $\hat{x}_0=2$. Upper curves $\tau=10$; lower curves $\tau=50$ ($\theta_s=0.2$ and $\alpha=0.3$). Due to the inhomogeneity of the diffusion coefficient, the density profile shows a tendency to skewness and it spreads preferentially towards the reference surface $\hat{x}=0$.

From Eq. (33), one has thus $V \sim \frac{3}{5} d_m \eta^{-1}$ in the range $\theta_s x \gg 1$ and $x \gg x_0$ (which implies $\eta \gg 1$). Hence, Eq. (32) can be approximated in this range by the equation

$$\partial_t \bar{n} = \frac{3}{5} d_m \nabla_\eta (\eta^{-1} \bar{n}) + d_m \nabla_\eta^2 \bar{n}. \quad (39)$$

The exact solution of Eq. (39) is

$$\bar{n}_{as}(\eta; \tau) = c (d_m \tau)^{-1/5} |\eta|^{-3/5} \exp\left(-\frac{\eta^2}{4 d_m \tau}\right), \quad (40)$$

where c is a constant of integration. Both Eqs. (39) and (40) are invalid around $\eta=0$. However, by expressing the result in terms of the variable x and by using $[1 + \theta_s^2 x^2]^{3/4} \sim (\frac{25}{4} \theta_s^3 |\eta|^3)^{1/5}$, Eq. (40) yields

$$n_{as}(x; \tau) = c (d_m \tau)^{-1/5} \exp\left(-\frac{1}{25} \frac{\theta_s^3 |x|^5}{d_m \tau}\right). \quad (41)$$

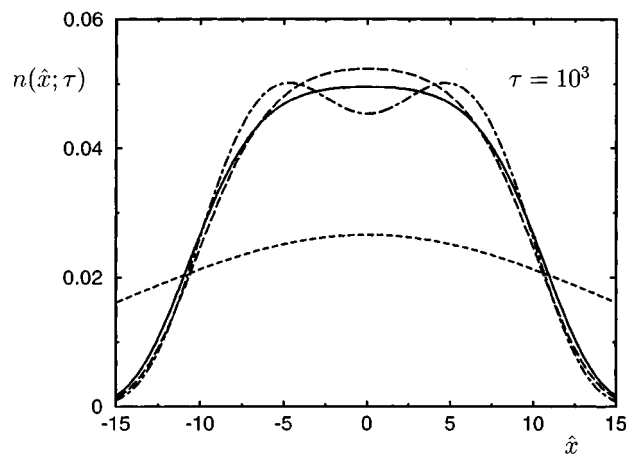


FIG. 3. The numerical solution of Eq. (28) (full line) is compared with the shearless (Gaussian packet) solution (dotted line) for $\tau=10^3$, $\theta_s=0.2$ and $\alpha=0.3$ ($\hat{x}_0=0$). Equation (37) (dot-dashed line) now exhibits two spurious maxima. Hence, Eq. (41) (dashed line) becomes a better approximation of the solution of Eq. (28).

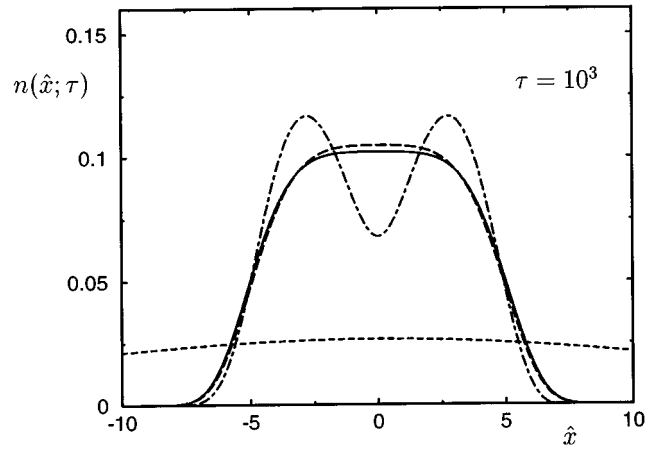


FIG. 4. The numerical solution of Eq. (28) (full line) is plotted against the shearless (Gaussian packet) solution (dotted line) for $\tau=10^3$, $\theta_s=0.8$ and $\alpha=0.3$ ($\hat{x}_0=0$). The dashed line is Eq. (41). The dot-dashed line represents the approximation (37).

This expression is nonsingular in $x=x_0$: It actually provides an approximation for the solution of Eq. (32) valid for all x when the latter has spread over a wide x -range (see Figs. 3 and 4). We also note that Eq. (41) is asymptotically compatible with the “generalized” Gaussian $\exp\{-x^2/D(\theta_s x)\tau\}$, which could be guessed from Eq. (28). Finally, the constant c is determined by the normalization constraint. One gets

$$c = \frac{5}{4\pi} \sqrt{\frac{2}{5 + \sqrt{5}}} \Gamma\left(\frac{4}{5}\right) (\sqrt{5} \theta_s^3)^{1/5}, \quad (42)$$

where $\Gamma(z)$ is the Gamma function. Equation (41) will be analyzed in Sec. VI B.

VI. THE VARIOUS STAGES OF DIFFUSION

We now analyze the behavior of the solution of Eq. (28). It can be divided into two distinct stages in which one uses either the solution (37) or the solution (41).

A. The quasi-Gaussian initial stage

Both the approximation (37) and the solution obtained from numerical simulation of Eq. (28) are plotted in Figs. 1 and 2 for two initial conditions x_0 and two values of τ . They are compared to the local Gaussian packet solution,

$$n_{\text{GAUS}}(x; \tau) = (4\pi D(\theta_s x_0) \tau)^{-1/2} \times \exp\left(-\frac{(x-x_0)^2}{4D(\theta_s x_0) \tau}\right). \quad (43)$$

If $x_0=0$, $D(\theta_s x_0)=d_m$ and Eq. (43) reduces to the usual Gaussian density profile in the absence of shear. For not too large values of τ , the absolute values of the factors entering the exponentials in Eq. (37) grow rapidly with $|x-x_0|$. Hence, the density profile is rather sharply centered around $x=x_0$. Due to the inhomogeneous diffusion coefficient which decreases with $|x|$ in Eq. (28), the density profile spreads slower (resp. faster) than n_{GAUS} away far from (resp. near to) the reference surface $x=0$. This effect can be characterized by the centered moments of the density profile (37),

$$\mu(\tau) \equiv \langle x(\tau) \rangle = \int_{-\infty}^{\infty} dx x n(x; \tau), \quad (44a)$$

$$\mu_p(\tau) \equiv \langle \delta x^p(\tau) \rangle = \int_{-\infty}^{\infty} dx [x - \mu(\tau)]^p n(x; \tau), \quad p \geq 2. \quad (44b)$$

Calculations are made easier by considering only $\theta_s x_0 \ll 1$. We then obtain the series expansions

$$\mu(\tau) = x_0 - 3d_m x_0 \tau \theta_s^2 + O(\theta_s^3), \quad (45a)$$

$$\mu_2(\tau) = 2d_m \tau \left\{ 1 - \frac{3}{2}(x_0^2 + 3d_m \tau) \theta_s^2 + O(\theta_s^3) \right\}. \quad (45b)$$

The shearless results are recovered from Eqs. (45) by setting $\theta_s = 0$. Due to the shear, diffusion decreases with distance from the reference surface $x=0$. Hence, a density profile centered initially in $x_0 \neq 0$ spreads preferentially towards the reference surface and the magnetic lines tend to be located on the average in $x=0$ [Eq. (45a) and Fig. 2]. Moreover, the spreading is in every case slower in sheared than in shearless systems [Eq. (45b)]. We also underscore that the expansions (45), which are time-dependent, obviously break down after a certain time τ_c . A rough estimation gives $\tau_c \approx 1/d_m \theta_s^2$; this limit will be confirmed in Sec. VI B. Finally, we note that Eq. (45b) yields a running ‘‘diffusion’’ coefficient,

$$\frac{1}{2} \frac{d}{d\tau} \mu_2(\tau) = d_m \left\{ 1 - \frac{3}{2}(x_0^2 + 6d_m \tau) \theta_s^2 + O(\theta_s^3) \right\}.$$

The *time-independent* part of this expression is the (dimensionless) expansion in θ_s of the wrong result, Eq. (8). Hence, Eq. (8) is an approximation of Eq. (45b) only for *small* τ . It does not provide the true asymptotic behavior (i.e. when $\tau \rightarrow \infty$) of μ_2 , as was naively assumed in the Corrsin-based treatment of Sec. II. The deviations from Gaussianity can be characterized by the coefficient of skewness and the kurtosis (or standardized fourth moment) defined, respectively, as

$$\gamma_3(\tau) = \mu_3(\tau) \mu_2^{-3/2}(\tau), \quad (46a)$$

$$\gamma_4(\tau) = \mu_4(\tau) \mu_2^{-2}(\tau). \quad (46b)$$

For the Gaussian packet, $\gamma_3=0$ and $\gamma_4=3$. On the contrary, we obtain, from Eq. (37),

$$\gamma_3(\tau) = -9 \frac{\sqrt{2}}{2} x_0 \sqrt{d_m \tau} \theta_s^2 + O(\theta_s^3), \quad (47a)$$

$$\gamma_4(\tau) = 3 \{ 1 - 4d_m \tau \theta_s^2 + O(\theta_s^3) \}. \quad (47b)$$

Equations (47) (also see Figs. 1 and 2) show that for small values of both α and θ_s , the deviations from Gaussianity remain weak, even for large τ . Due to the limit $\tau \ll 1/d_m \theta_s^2$, however, the density profile (37) does not describe the truly asymptotic behavior (i.e. for $\tau \rightarrow \infty$) of the solution of Eq. (28).

B. The strongly anomalous asymptotic stage

In Figs. 3 and 4, we plotted the numerical solution of Eq. (28) and the density profile (41) for very large values of τ (Fig. 5, where $x_0=2$ shows how the memory of the initial

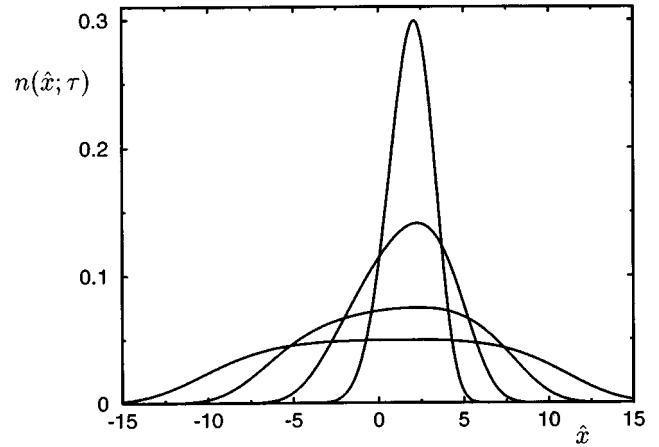


FIG. 5. The numerical solution of Eq. (28) for $\hat{x}_0=2$ is represented for successive times $\tau=10, \tau=50, \tau=250$ and $\tau=10^3$ (here $\theta_s=0.2$ and $\alpha=0.3$). The memory of the initial condition \hat{x}_0 is slowly lost.

condition is asymptotically lost). Two different values of θ_s have also been considered. Clearly, the deviations from Gaussianity are now essential. Figures 3 and 4 also show Eq. (37), which, obviously, no longer provides a relevant approximation of the solution of Eq. (28). In particular, Eq. (37) exhibits two maxima, which is a spurious feature. The moment at which these two maxima appear can be used to characterize the transition from the quasi-Gaussian stage, considered in Sec. VI A, to the asymptotic non-Gaussian stage. Let us make this more precise in the case $x_0=0$, which yields generic results for sufficiently long times. The derivative of Eq. (37) can then be approximated by its series expansion in $\theta_s x$, which is proportional to

$$\frac{d}{dx} n \propto (3d_m \theta_s^2 \tau - 2)x - 2\theta_s^2 x^3 + O(\theta_s^4 x^4). \quad (48)$$

Equation (48) admits nontrivial solutions $x_{(\pm)} = \pm \theta_s^{-1} \sqrt{\frac{3}{2} d_m \theta_s^2 \tau - 1}$, yielding the spurious maxima of Eq. (37), only if $\tau > \tau_c$, with

$$\tau_c = \frac{2}{3d_m \theta_s^2}. \quad (49)$$

It confirms the estimation of Sec. VI A. The transition time τ_c can be very large when both α and θ_s are small. The non-Gaussian stage is characterized from the behavior of the first two moments (44) of the solution (41). They are

$$\mu = 0, \quad (50a)$$

$$\mu_2(\tau) = \frac{5^{13/10}}{2\pi} \sqrt{\frac{2}{5+\sqrt{5}}} \Gamma\left(\frac{4}{5}\right) \Gamma\left(\frac{3}{5}\right) \left(\frac{d_m \tau}{\theta_s^3}\right)^{2/5}, \quad \tau \rightarrow \infty. \quad (50b)$$

Equation (50b) implies an effective *subdiffusive* asymptotic behavior. Consequently, the shearless limit $\theta_s \rightarrow 0$ (i.e. $L_s \rightarrow \infty$) is singular. The skewness parameter (46a) and the kurtosis (46b) behave like

$$\gamma_3 = 0, \quad (51a)$$

$$\gamma_4 = \sqrt{\frac{2}{5}} \frac{\sqrt{5 + \sqrt{5}}}{\Gamma(4/5)\Gamma(3/5)^2} \approx 2.07, \quad \tau \rightarrow \infty. \quad (51b)$$

Both the skewness parameter and the kurtosis are thus asymptotically independent of α and θ_s . Moreover, γ_4 is approximately 72% of the Gaussian one.

VII. DISCUSSION

The statistical behavior of magnetic lines has been investigated for a sheared main magnetic field presenting a stochastic component in the $x-y$ plane. A Liouville equation is associated with the equations of motion for the magnetic lines. The Liouville equation is averaged over an ensemble of realizations of the magnetic field. Within the quasilinear approximation, it yields a convection-diffusion equation for the probability distribution function. Due to finite shear, the diffusion coefficients are space-dependent functions peaked around the reference surface $x=0$ with scaling $x\lambda_{\parallel}/L_s\lambda_{\perp}$. It implies that the shear slows down the “diffusion” of the magnetic lines away from $x=0$. The importance of this effect must be underscored. Indeed, even when $x/L_s \ll 1$, one usually has $\lambda_{\parallel}/\lambda_{\perp} \gg 1$, which makes the ratio $x\lambda_{\parallel}/L_s\lambda_{\perp}$ unconstrained. Hence, the effects of the shear can be significant, even in regions along the x -axis close to the reference surface (in the sense $x/L_s \ll 1$). Two diffusion stages can be distinguished: First, a quasi-Gaussian stage is observed, during which the density profile spreads with a rate (roughly) proportional to the local value of the diffusion coefficient $D(x_0\lambda_{\parallel}/L_s\lambda_{\perp})$. The latter is in any case smaller in sheared than in shearless systems. This initial stage occurs during an effective time (i.e. for a length along z), which might be very long. However, the actual asymptotic stage is definitely non-Gaussian. The memory of the initial condition x_0 has then been lost and the density profile becomes symmetrically centered around the reference surface $x=0$. The latter can thus be seen as an “attractor” for the system. During this final stage the spreading is very slow, which leads to an effective subdiffusive behavior for the magnetic lines.

It is important to note that the Langevin approach is not appropriate for studying such subdiffusive behavior in sheared systems because of the non-Gaussian property. It is indeed impossible to get from the convection-diffusion equation a closed set of equations for the first two moments of the PDF. Moreover, the space-dependent diffusion tensor cannot, in such inhomogeneous systems, be deduced from the second moment. Another important consequence is that the Corrsin (or independence) approximation breaks down and, hence, must be relaxed. Indeed, this latter approximation implies that any Eulerian statistical property, like Gaussianity, is also observed in the Lagrangian picture, which is wrong in the present case.

Finally, let us consider the impact of these results for transport, i.e. when particles and collisions are included. Obviously, the asymptotic subdiffusive nature of the line spreading will influence the particle motion only if the particle sticks to the same magnetic line for enough z -length. As we know that the subdiffusion of the line occurs after a rather long z -path, this situation will happen for low perpendicular collision frequency ν , typically $\nu \lesssim 1/\lambda_{\parallel}\tau_c$ [see Eq. (49)]. In the opposite limit of rather high perpendicular collision frequency, a particle will jump from a line to another before any subdiffusive spreading of the line. However, even in this case, the diffusion coefficient is locally smaller in a sheared system. We can thus expect the shear to slow down the spreading of the particles too. We intend to consider more deeply these questions in a forthcoming publication.

ACKNOWLEDGMENTS

Interesting discussions with J. H. Misguich and H.-D. Wang are acknowledged. We thank D. Carati and A. Grecos for fruitful comments.

The work of E.V.E. is supported by the “Fonds pour la Formation par la Recherche dans l’Industrie et dans l’Agriculture” (FRIA), Belgium.

- ¹P. Liewer, Nucl. Fusion, **22**, 543 (1985).
- ²M. N. Rosenbluth, R. Z. Sagdeev, J. B. Taylor, and G. M. Zaslavsky, Nucl. Fusion, **6**, 297 (1966).
- ³A. A. Galeev and L. M. Zelenyi, Plasma Phys. Controlled Fusion **14**, 249 (1971).
- ⁴T. H. Stix, Phys. Rev. Lett. **30**, 833 (1973).
- ⁵T. H. Stix, Nucl. Fusion **18**, 354 (1978).
- ⁶A. B. Rechester and M. N. Rosenbluth, Phys. Rev. Lett. **40**, 38 (1978).
- ⁷J. H. Krommes, Progr. Theor. Phys. Suppl. **64**, 137 (1978).
- ⁸B. B. Kadomtsev and O. P. Pogutse, in *Plasma Physics and Controlled Nuclear Fusion Research*, Proceedings of the 7th International Conference, Innsbruck, 1978 (International Atomic Energy Agency, Vienna, 1979), Vol. 1, p. 649.
- ⁹P. H. Diamond, T. H. Dupree, and D. J. Tetreault, Phys. Rev. Lett. **45**, 562 (1980).
- ¹⁰F. A. Haas, A. Thyagaraja, and I. Cook, Plasma Phys. **23**, 1027 (1981).
- ¹¹H. A. Rose, Phys. Rev. Lett. **48**, 260 (1982).
- ¹²J. A. Krommes, C. Oberman, and R. G. Kleva, J. Plasma Phys. **30**, 11 (1983).
- ¹³G. Zimbaro, P. Veltri, and F. Malara, J. Plasma Phys. **32**, 141 (1984).
- ¹⁴A. Thyagaraja and F. Haas, Phys. Scr. **31**, 83 (1985).
- ¹⁵M. B. Isichenko, Plasma Phys. Controlled Fusion **33**, 795 (1991).
- ¹⁶M. B. Isichenko, Plasma Phys. Controlled Fusion **33**, 809 (1991).
- ¹⁷J. M. Rax and R. B. White, Phys. Rev. Lett. **68**, 1523 (1992).
- ¹⁸M. Coronado, E. J. Vitela, and A. Akcasu, Phys. Fluids B **4**, 3935 (1992).
- ¹⁹J. R. Myra, P. J. Catto, H. E. Mynick, and R. E. Duvall, Phys. Fluids B **5**, 1160 (1993).
- ²⁰G. Laval, Phys. Fluids B **5**, 711 (1993).
- ²¹R. B. White and Y. Wu, Plasma Phys. Controlled Fusion **35**, 595 (1993).
- ²²L. Hannibal, Phys. Fluids B **5**, 3551 (1993).
- ²³H. Sugimoto, T. Kurasawa, and H. Ashida, Plasma Phys. Controlled Fusion **36**, 383 (1994).
- ²⁴H.-D. Wang, M. Vlad, E. Vanden Eijnden, F. Spineanu, J. H. Misguich, and R. Balescu, Phys. Rev. E **51**, 4844 (1995).
- ²⁵E. Vanden Eijnden and R. Balescu, J. Plasma Phys. **54**, 185 (1995).
- ²⁶S. Corrsin, in *Atmospheric Diffusion and Air Pollution*, edited by F. N. Frenkiel and P. A. Sheppard (Academic, New York, 1959), p. 161.
- ²⁷J. Weinstock, Phys. Fluids **19**, 11 (1976).
- ²⁸W. D. McComb, *The Physics of Fluid Turbulence* (Clarendon, Cambridge, 1991).

- ²⁹N. G. van Kampen, *Stochastic Processes in Physics and Chemistry* (North-Holland, Amsterdam, 1992).
- ³⁰C. W. Gardiner, *Handbook of Stochastic Methods* (Springer-Verlag, Berlin, 1985).
- ³¹H. Risken, *The Fokker-Planck Equation*, Springer Series in Synergetics 18 (Springer-Verlag, Berlin, 1989).
- ³²A simple example of noise induced drift is given by the stochastic oscillator (or Kubo oscillator) $\dot{x} = iax$, where a is a time-independent Gaussian variable, $\langle a \rangle = 0$, $\langle a^2 \rangle = A^2$. It yields indeed $\langle x(t) \rangle = x_0 \exp(-A^2 t^2) \neq x_0$.
- ³³R. Balescu, H.-D. Wang, and J. H. Misguich, *Phys. Plasmas* **1**, 3826 (1994).
- ³⁴R. Bourret, *Nuovo Cimento* **26**, 1 (1962).
- ³⁵A. Brissaud and U. Frisch, *J. Math. Phys.* **15**, 524 (1974).
- ³⁶M. V. Smoluchowski, *Ann. Phys.* **48**, 1103 (1915).
- ³⁷A. H. Nayfeh, *Perturbation Methods* (Wiley, New York, 1973).
- ³⁸For mathematical purposes, the physical restriction $\theta_s \leq 1$ is unnecessary here.